Fabrication of wide-bandgap β-Cu(In,Ga)$_3$Se$_5$ thin films and their application to solar cells

Ji Hye Kim[1] · Young Min Shin[1] · Seung Tae Kim[1] · HyukSang Kwon[1] · Byung Tae Ahn[1]*

[1]Department of Materials Science and Engineering, Korea Advanced Institute of Science and Technology, Daejeon 305-701, Korea

ABSTRACT: Cu(In,Ga)$_3$Se$_5$ is a candidate material for the top cell of Cu(In,Ga)Se$_2$ tandem cells. This phase is often found at the surface of the Cu(In,Ga)Se$_2$ film during Cu(In,Ga)Se$_2$ cell fabrication, and plays a positive role in Cu(In,Ga)Se$_2$ cell performance. However, the exact properties of the Cu(In,Ga)$_3$Se$_5$ film have not been extensively studied yet. In this work, Cu(In,Ga)$_3$Se$_5$ films were fabricated on Mo-coated soda-lime glass substrates by a three-stage co-evaporation process. The Cu content in the film was controlled by varying the deposition time of each stage. X-ray diffraction and Raman spectroscopy analyses showed that, even though the stoichiometric Cu/(In+Ga) ratio is 0.25, Cu(In,Ga)$_3$Se$_5$ is easily formed in a wide range of Cu content as long as the Cu/(In+Ga) ratio is held below 0.5. The optical band gap of Cu$_{0.3}$(In$_{0.65}$Ga$_{0.35}$)$_3$Se$_5$ composition was found to be 1.35eV. As the Cu/(In+Ga) ratio was decreased further below 0.5, the grain size became smaller and the band gap increased. Unlike the Cu(In,Ga)Se$_2$ solar cell, an external supply of Na with Na$_2$S deposition further increased the cell efficiency of the Cu(In,Ga)$_3$Se$_5$ solar cell, indicating that more Na is necessary, in addition to the Na supply from the soda lime glass, to suppress deep level defects in the Cu(In,Ga)$_3$Se$_5$ film. The cell efficiency of CdS/Cu(In,Ga)$_3$Se$_5$ was improved from 8.8 to 11.2% by incorporating Na with Na$_2$S deposition on the CIGS film. The fill factor was significantly improved by the Na incorporation, due to a decrease of deep-level defects.

Key words: Cu(In,Ga)$_3$Se$_5$, β-CIGS, external Na supply, wide-band gap absorber, deep level defects

Nomenlature

α-CIGS : Cu(In,Ga)Se$_2$

β-CIGS : Cu(In,Ga)$_3$Se$_5$

V_{oc} : open cirduit voltage, V

J_{sc} : short circuit current, mA/cm^2

FF : fill factor

η : conversion efficiency, %

substript

XRD : x-ray diffraction

SEM : scanning electron micorscopy

AES : Auger electron spectroscopy

QE : quantum efficiency

LTPL : low temperature photoluminescence

1. Introduction

Chalcopyrite Cu(In,Ga)Se$_2$ (α-CIGS) and related films are gaining considerable interest for photovoltaic devices since their high optical absorption coefficient and adjustable band gap can enable to achieve a high conversion efficiency in α-CIGS solar cells. Technical advances in α-CIGS solar cells involving the co-evaporation of Cu, In, Ga, and Se elements through a three-stage process have reached the highest efficiency of over 20% in thin film solar cells[1]. Solar cells with α-CIGS film show the highest efficiency with a relatively narrow band gap energy of 1.2 eV, which is below the optimum value of 1.4 eV. As the band gap of absorber materials increases, the open circuit voltage of cells deviates from being expected, resulting in the lower efficiency from theoretical values[2].

Recently, a tandem structure is proposed to improve the efficiency above 25%. In the structure, top cell consists of wide band gap light absorber and bottom cell consists of narrow band gap light absorber. The efficiency is high enough for bottom cell with band gap 1.0 eV. But a wide band gap absorber for top cell has not been developed yet. The purpose of our work is to find a light absorber applicable to top cell in the tandem structure.

$CuIn_3Se_5$ (β-CIGS) phase is a candidate for top cell absorber because the phase shows larger band gap than $CuInSe_2$ (E_g=0.9 eV)[3]. The $CuIn_3Se_5$ phase contains more In than Cu, resulting in the increase of band gap because of stronger In-Se bonding than Cu-Se bonding. The β-CIGS phase is often found on the surface of α-CIGS film because of excess supply of In, Ga and Se during the three-stage co-evaporation process. The existence of this phase greatly enhances the device performance of $CuInSe_2$ solar cell[4]. It is believed that $CuInSe_2$ phase on the CIGS surface can reduce the conduction band offset at the CdS/CIGS interface[5]. The band gap of the $CuInSe_2$ phase can be increased by adding Ga or S, suggesting that this material has a potential for top cell.

Even though there were a few early work reported, the β-CIGS film has not been well characterized yet[6]. It is worthwhile to revisit the film for efficiency improvement of the cell with β-CIGS film for the purpose of tandem cells and for higher efficiency in single junction α-CIGS solar cells. In this research, β-CIGS films were prepared by three-stage co-evaporation process and the photovoltaic properties of CdS/β-CIGS cell were investigated by controlling the Ga content and by adding supplying more Na from Na_2S source.

2. Experimental

CIGS films were grown on a Mo-costed soda-lime glass substrate by the three-stage co-evaporation process. In the first stage, an $(In,Ga)_2Se_3$ film was deposited at 350°C by co-evaporating In, Ga and Se. In the second stage, the substrate temperature was elevated to 550°C in 5 min and Cu and Se were co-evaporated. At this stage, a CIGS film was formed in situ by interaction of the $(In,Ga)_2Se_3$ film and the evaporated Cu and Se. In the third stage, In, Cu, and Se sources were co-evaporated on the CIGS films. The overall composition was controlled by adjusting the deposition time and evaporation rates.

The thickness of the film was about 2 μm. The CIGS films were characterized using XRD, Raman spectroscopy, AES, and SEM. UV-spectroscopy measurements were performed to verify optical transmittance of films deposited in glass substrates. Defects in CIGS film were analyzed by LTPL at 10K.

Solar cells with ZnO/CdS/β-CIGS structure were fabricated on a Mo-coated soda-lime glass substrate. The Mo back contact layer with a thickness of 1 μm was deposited by dc magnetron sputtering. The CdS buffer layer with a thickness of 50 nm was deposited by chemical bath deposition. The ZnO window layer was deposited by rf magnetron sputtering and it consisted of 50-nm thick intrinsic ZnO and 400-nm thick Al-doped ZnO. The photovoltaic properties of solar cells were assessed at AM1.5, 100 mW/cm^2 illumination.

3. Results

Fig. 1(a) shows XRD patterns of CIGS thin films grown on Mo coated soda-lime glass substrate with various Cu contents in the Cu(In,Ga)Se system. The Cu/(In+Ga) ratio varies from 0.80 to 0.30. Since the XRD patterns of α-CIGS and β-CIGS are very similar, it is not easy to distinguish β-CIGS phase from α-CIGS phase. However the (112) peak moves to larger angle as the Cu content decreases as shown in Fig. 1(b). When the Cu content is below 0.47, the (112) peak is fixed and does not increase where β-CIGS phase is formed. Moreover when the content is 0.29, an additional (110) peak appears, corresponding to β-CIGS phase[7, 8]. Even though the In and Ga contents are large in the β-CIGS film, no secondary phase such as In_2Se_3 or Ga_2Se_3 exists. The structure of the compound is a tetragonal and a polycrystalline with (112) preferred orientation.
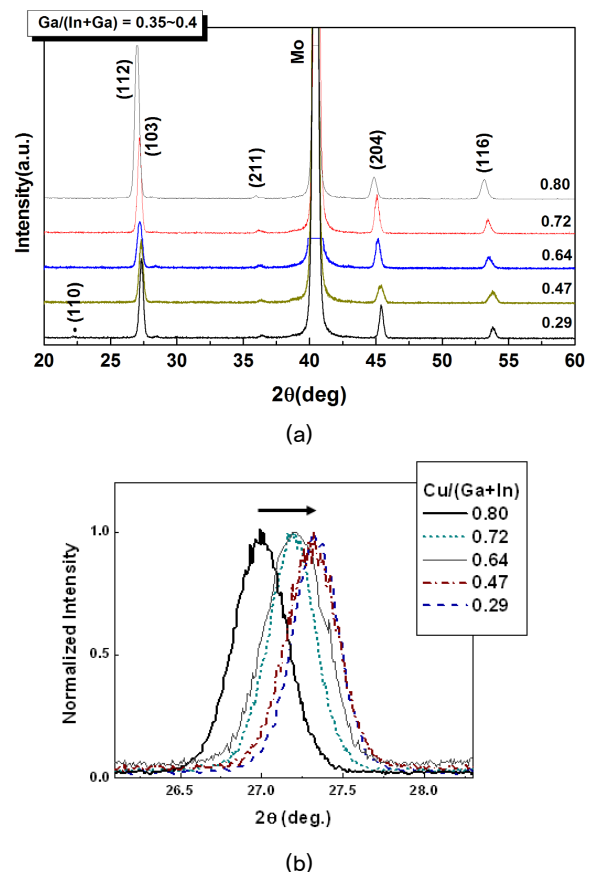

(a)

(b)

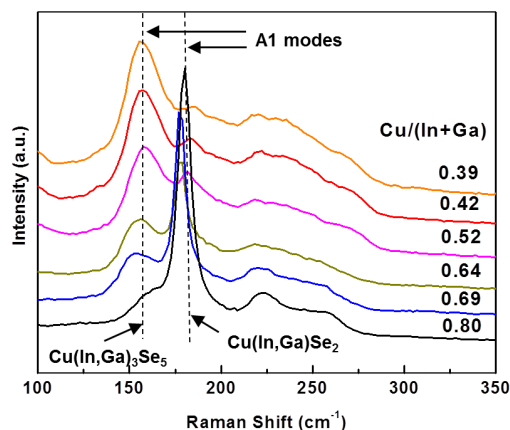**Fig. 1.** XRD patterns (a) and (112) peaks (b) of Cu(In,Ga)Se films with various Cu contents.

Fig. 2. Raman spectroscopy of Cu(In,Ga)Se films with various Cu contents. The A1 modes of Cu(In,Ga)$_3$Se$_5$ and Cu(In,Ga)Se2 are clearly distinguishable.
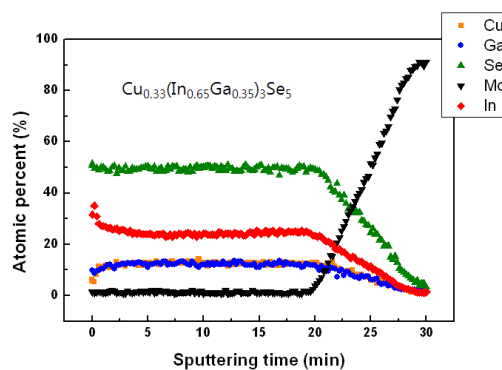

Fig. 3. SEM morphologies of Cu(InGa)Se films with the Cu content of (a)0.72, (b)0.64, (c)0.47, (d)0.30.

Fig. 4. AES depth profile of Cu(In,Ga)3Se5 film.

Fig. 5. Optical transmittance of Cu(In,Ga)Se films with various Cu contents and Ga/(Ga+In)=0.35. Two different absorption edges are clearly seen.

The α-CIGS and β-CIGS phases are more clearly distinguished in Raman spectroscopy as shown in Fig. 2. When the Cu contents is below 0.5, the β-CIGS phase is clearly dominant. Apparently a small amount of β-CIGS phase exists in the α-CIGS film with the Cu content of above 0.5.

The effects of the Cu content on the microstructure of CIGS thin film are shown in cross sectional SEM images (Fig. 3). As the Cu contents decreases, the grain size in the film after the third stage became smaller. In the plane-view SEM images, faceted and tightly connected grains are grown on the surface.

The effects of the Cu content on the microstructure of CIGS thin film are shown in cross sectional SEM images (Fig. 3). As the Cu contents decreases, the grain size in the film after the 3rd stage became smaller. In the plane-view SEM images, faceted and tightly connected grains are grown on the surface.
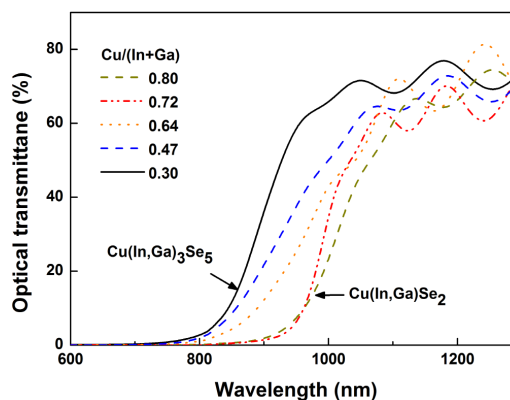
Fig. 4 is the AES depth profile of the β-CIGS film with Cu$_{0.33}$(In$_{0.65}$Ga$_{0.35}$)$_3$Se$_5$ composition. Each element is uniformly distributed in the film, which indicates β-CIGS phase was formed through the entire depth of the film by the three-stage co-evaporation process. Also we confirmed that the film does not have multi-phases but a single phase.

The optical transmittance of the CIGS thin film with various Cu contents ranging from 0.8 to 0.3 is shown in Fig. 5. The absorption edges of CIGS thin films with lower Cu contents move to shorter wavelength and also exhibit higher transmittance in long wavelength region. Two different absorption edges are clearly seen with various Cu contents. Also the high transmittance in the long wavelength region is higher in β-CIGS film, which is desirable for tandem structure because bottom cell should absorb more long wavelength lights.

Absorption coefficients were determined by measuring both the transmittance and reflectivity of the Cu(In,Ga)Se films. The $(ah\nu)^2$ of a β-CIGS film plotted as a function of photon-energy

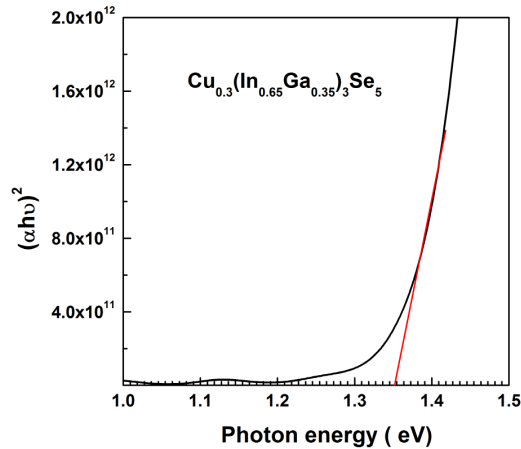**Fig. 6.** Variation of (ahv)^2 of Cu(In,Ga)$_3$Se$_5$ film as a function of photon energy (hv).
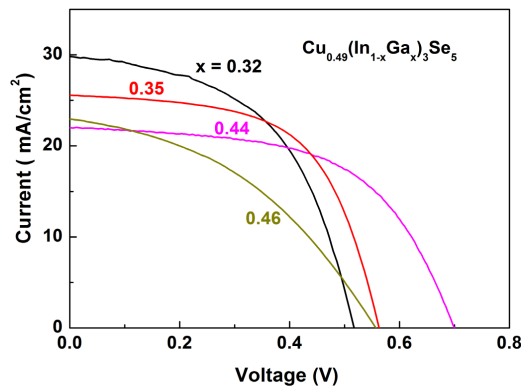
Fig. 7. Illuminated J-V characteristics of solar cells fabricated using the CIGS-based films.

Table 1. Photovoltaic parameters of Cu$_{0.49}$(In,Ga)$_3$Se$_5$ solar cells with various Ga contents.

Ga/(In+Ga)	V_{oc}(V)	J_{sc}(mA/cmP)	FF	η(%)
0.32	0.52	29.9	0.53	8.1
0.35	0.56	25.6	0.59	8.5
0.44	0.70	22.0	0.63	8.8
0.49	0.66	17.2	0.44	5.0
0.42(with Na$_2$S)	0.67	24.5	0.68	11.2
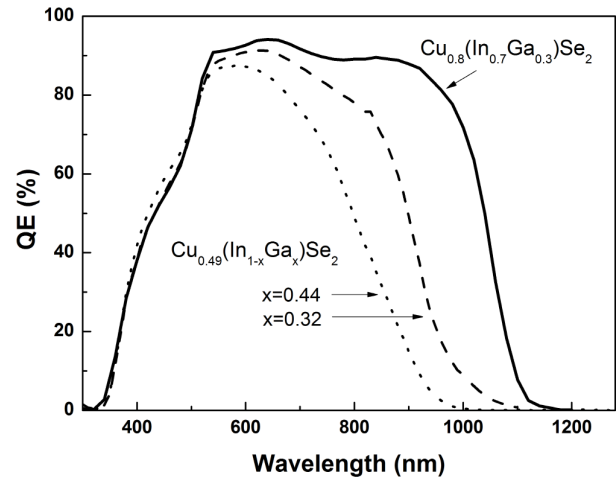
Fig. 8. Spectral quantum efficiency of CIGS solar cells.

(hv) in Fig. 6 showed a straight-line. It indicates that the optical absorption of β-CIGS phase occurs by a direct band gap transition. The band gap was estimated to 1.35 eV from extrapolating intercept. On the other hand, the E_g does not change significantly while the transmittance greatly increases when the Cu content changes from 0.8 to 0.3. The higher optical transmittance might be due to less light scattering of In and Ga atoms compared to Cu atoms, indicating that it is useful for top cell of tandem cells.

Fig. 7 shows the illuminated J-V curves of CdS/β-CIGS solar cells with various Ga contents in the area of 0.44cm^2. The Cu/(In+Ga) ratio was about 0.49. The conversion efficiency increased from 8.1% to 8.8% as the Ga/(In+Ga) ratio increases from 0.31 to 0.44. However, the efficiency was significantly lowered by further increase of the Ga content. As the Ga content increased the short circuit current was lowered and the open circuit voltage was increased as expected except Ga/(In+Ga)= 0.49. The photovoltaic parameters such as V_{oc}, J_{sc}, FF, and η are summarized in Table 1.

The increase of Ga in the CIGS film increases the band gap and may reduce defect concentrations, according previous reports.[9] However, too much addition of Ga always showed an adverse effect.

The reason of adverse effect was due to poor morphology with too small grains and probably due to the formation of Ga$_{Cu}$ antisite which is assumed to be a deep-level trap center.

Fig. 8 shows the spectral quantum efficiency (QE) of β-CIGS solar cells with Ga contents of 0.35 and 0.44. For comparison the QE of α-CIGS solar cell with a Cu(In$_{0.70}$Ga$_{0.30}$)Se$_2$ composition was added. The cut-off wavelength shifted to shorter wavelengths due to different band gap from α-CIGS to β-CIGS. The band gap of β-CIGS cell with Ga content of 0.44 is increased to 1.4 eV, estimated from the cut-off wavelength. The increase of QE value of the β-CIGS near the cut-off wavelength is rather slow compared to that of α-CIGS cell.

Even though we used soda-lime glass as a substrate, the role of sodium in the β-CIGS cell should be more clearly addressed. For the purpose, sodium was further supplied into β-CIGS film by the thermal deposition of Na$_2$S on Mo film or on CIGS film during the film preparation. The small amount of sodium into the CIGS absorber layer leads beneficial effects on performance
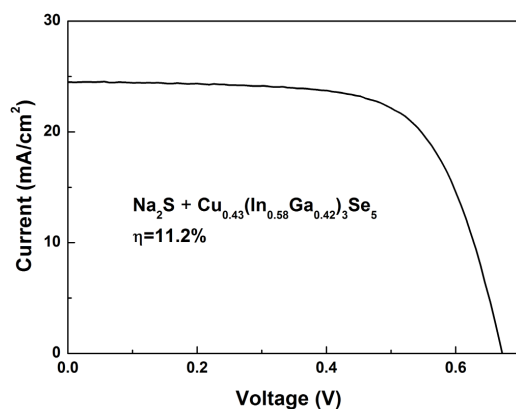
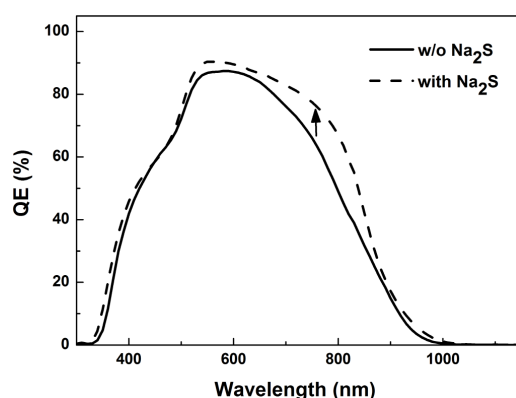**Fig. 9.** Illuminated J-V curves of Cu(In,Ga)3Se5 solar cell fabricated by adding an Na2S film on CIGS film.

Fig. 10. Spectral quantum efficiency of $Cu(In,Ga)_3Se_5$ solar cells with and without Na_2S incorporation.

of solar cell devices[10]. The improved conversion efficiencies mainly by enhancing the fill factor and open circuit voltage of the devices[11, 12], or increased p-type conductivity observed for sodium containing devices[12, 13].

Fig. 9 shows a J-V curves of β-CIGS solar cells fabricated by adding an Na_2S layer on CIGS film where Cu/(In+Ga)=0.43 and Ga/(In+Ga)=0.42. The conversion efficiency was improved from 8.8% to 11.2% by adding Na in CIGS with Na_2S. The percent of conversion efficiency increase is as much as 27%. In the cell with Na external doping, V_{oc}, J_{sc}, and FF are 0.67 V, 24.49 mA/cm^2, and 0.68, respectively, for an active layer of 0.44 cm^2. Note that the FF is greatly increased from 0.63 to 0.68, compared to FF values in Table 1. We still have more room to improve it, up to 0.78. So far the record efficiency of β-CIGS cell is 12.2% by AGU team[6].

Fig. 10 shows the external quantum efficiencies measured for solar cells using CIGS-based absorber layers without and with Na_2S. The cut-off wavelength in the near-infrared regions does not shift. In the wavelength region from 550 to 900 nm the QE
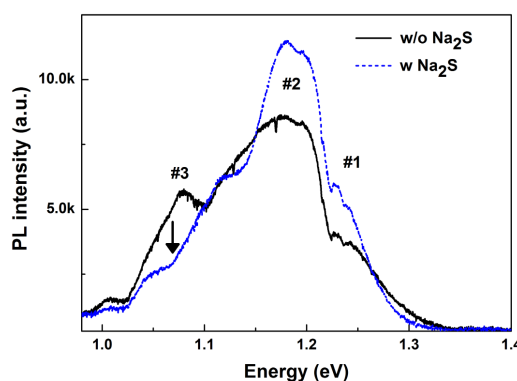

Fig. 11. LTPL of Cu(In,Ga)3Se5 films without and with Na2S incorporation.

value increases successively for the sample with Na_2S incorporation. The result suggest that the diffusion length of excess carrier is larger, probably due to the suppression of In_{Cu} and Ga_{Cu} antisites defects by Na incorporation.

We found that the resistivity of the CIGS film without Na external supply rapidly increased as the Cu/(In+Ga) ratio decreased. However, it was observed that the resistivity was decreased by the supply of Na with Na_2S. It suggests that the presence of Na suppressed the formation of donor type defects such as In_{Cu} and Ga_{Cu} antisites, resulting in the decrease of charge compensating by the deep level defect and leading to higher hole concentration in β-CIGS film.

Fig. 11 shows the LTPL spectra of β-CIGS films without and with Na_2S incorporation. The three emissions peaks are observed at the energy of 1.24 (#1) and 1.19 (#2), and 1.08eV (#3). The #3 emission peak is likely originated from deep level defect, probably due to antisites such as In_{Cu} or Ga_{Cu}. However, the exact indentification of defects is not a simple task at the moment. However, note that the intensity of peak #3, that is originated form deep level defects, was substantially reduced by Na_2S incorporation. The explanation of point defects in the film is not well understood yet and it is beyond the scope of this paper.

Even though the efficiency of β-CIGS cell is much smaller than that of α-CIGS cell, our results provide important information. The efficiency could be improved by reducing the deep level defects with external Na incorporation. The resistance of the film is lowered and the FF was improved. We believe that the performance of solar cell will be further improved by reducing the deep level defects by careful design of process conditions and band structure at the CdS/β-CIGS interface.

4. Conclusions

Defect chalcopyrite $Cu(In.Ga)_3Se_5$ films have been prepared by a three-stage co-evaporation process. As the Cu/(In+Ga) ratio decreased below 0.5, a $Cu(In,Ga)_3Se_5$ phase was easily formed. In the $Cu(In,Ga)_3Se_5$ film, the transmittance in the wavelength region just above the absorption edge was noticeably higher, which indicates that the film can be a good candidate for wide band gap absorber. The conversion efficiency of $Cu(In_{0.58}Ga_{0.42})_3Se_5$ cell was improved from 8.8 to 11.2% by supplying external supply of Na using Na_2S deposition. The incorporation of Na reduced the LTPL intensity of deep level defects, resulting in the decrease of resistivity of $Cu(In.Ga)_3Se_5$ film. To improve the cell efficiency further, it is necessary to reduce deep level defects and design an optimum band structure at the $CdS/Cu(In.Ga)_3Se_5$ interface.

Acknowledgment

References

1. P. Jackson, D. Hariskos, E. Lotter, S. Paetel, R. Wuerz, R. Menner, W. Wischmann, M. Powalla, "New world record efficiency for $Cu(In,Ga)Se_2$ thin-film solar cells beyond 20%", Prog. Photovolt: Res. Appl., Vol. 19, pp. 894–897, 2011.
2. M. Gloeckler, J.R. Sites, "Efficiency limitations for wide-band-gap chalcopyrite solar cells", Thin Solid Films, Vol. 480-481, pp. 241-245, 2005.
3. T. Negami, N. Kohara, M. Nishitani, T. Wada, "Preparation of ordered vacancy chalcopyrite-type $CuIn_3Se_5$ thin films", Jpn. J. Appl. Phys., Vol. 33, pp. L1251 - L1253, 1994.
4. D. Y. Lee, J. J. Yun, K. H. Yoon, B. T.Ahn, "Characterization of Cu-poor surface on Cu-rich $CuInSe_2$ film prepared by evaporating binary selenide compounds and its effect on solar efficiency", Thin Solid Films, Vol. 410, pp171-176, 2002.
5. L. Larina, D. Shin, J. H. Kim, B. T. Ahn, Energy Environ. Sci., "Alignment of energy levels at the $ZnS/Cu(In,Ga)Se_2$ interface" Vol.4, pp 3487-3493, 2011.
6. T. Nakada, T. Mouri, Y. Okano, A. Kunioka, "$Cu(In,Ga)_3Se_5$-based thin film solar cells fabricated by Na ontrol technique", 14th EU-PVSEC, pp. 2143, 1997.
7. M. A. Contreras, H. Wiesner, J. Tuttle, K. Ramanathan, R. Noufi, "Issues on the chalcopyrite/defect-chalcopyrite junction model for high-efficiency $Cu(In,Ga)Se_2$ solar cells", Sol. Energ. Mater. Sol. Cells, Vol. 49, pp. 239-247, 1997.
8. E. Schmid, M. Ruckh, F. Grunwald, and H.W. Schock, "Chalcopyrite/defect chalcopyrite heterojunctions on the basis of CuInSe2", J. Appl. Phys., Vol. 73, No. 6, pp. 2902, 1993.
9. G. Hanna, A. Jasenek, U. Rau, H.W. Schock, "Influence of the Ga-content on the bulk defect densities of $Cu(In,Ga)Se_2$", Thin Solid Films, Vol. 387, pp. 71-73, 2001.
10. J. Hedstrom, M. Bodegard, A. Kylner, L. Stolt, D. Hariskos, and H. W. Schock, "$ZnO/CdS/Cu(In,Ga)Se_2$ thin film solar cells with improved performance", Proceedings of the 23rd IEEE–PVSC, pp. 364, 1993.
11. M. A. Contreras, B. Egaas, P. Dippo, J. Webb, J. Granada, K. Ramanathan, S. Ashher, A. Swartzlander, and R. Noufi, "On the role of Na and modifications to CIGS absorber materials using Thin MF (M=Na,K,Cs) precursor layers", Proceedings of 26th IEEE-PVSC, pp. 359-362, 1997.
12. K. Granath, M. Bodegard, and L. Stolt, "The effect of NaF on $Cu(In, Ga)Se_2$ Thin film solar cells", Sol. Energy Mater. Sol. Cells, Vol. 60, pp. 279-293, 2000.
13. M. Ruckh, D. Schmid, M. Kaiser, R. Schaffler, T. Walter, and H.W. Schock, "Influence of substrates on the electrical properties of $Cu(In,Ga)Se_2$ thin films", Proceedings of 1st WCPEC, pp.156-159, 1994.